Nitric Oxide 93 (2019) 15–24

Contents lists available at ScienceDirect

Nitric Oxide

journal homepage: www.elsevier.com/locate/yniox

Comprehensive study of nitrofuroxanoquinolines. New perspective donors of NO molecules

Nikita S. Fedik, Mikhail E. Kletskii, Oleg N. Burov*, Anton V. Lisovin, Sergey V. Kurbatov, Vladimir A. Chistyakov, Pavel G. Morozov

Department of Chemistry, Southern Federal University, 7, Zorge St., Rostov-on-Don, 344090, Russia

A B S T R A C T

The goal of present work is the study of NO releasing mechanisms in nitrofuroxanoquinoline (NFQ) derivatives. Mechanisms of their structural non-rigidity and pathways of NO donation - spontaneous or under the action of sulfanyl radicals or photoirradiation - were considered in details, both experimentally and quantum chemically. Furoxan-containing systems of the discussed type are not capable of spontaneous or photoinduced decomposition under mild conditions, and sulfanyl (radical) induced processes are the most preferable. It was shown that appropriate modification of NFQ through [3 + 2] cycloaddition and subsequent aromatization is a powerful tool to design new prospective donors of NO molecule. Two newly obtained NFQ derivatives were proven to have unusually high NO activity in full accordance with the theoretical model. We hope that these examples will encourage community to seek for new NO active molecules among cycloadducts and modified furoxanes.

1. Introduction

Nitrogen (II) oxide is a multimodal regulator of various physiological processes (relaxation of vessels, thrombocyte aggregation inhibition, immune and nervous system operation), and also pathological conditions in a human organism (inflectional, inflammatory, and tumorous diseases) [1–3]. In this regard, synthesis of new exogenous NO-donors is one of the priority tasks of medicinal chemistry.

In a series of such compounds derivatives of nitrobenzofuroxans (nitrobenzoxadiazoles) with a wide range of biological activity, driven by their NO-donor properties, stand out [4,5]. Furoxan derivatives are also efficient against tuberculosis bacteria [6], could serve as inflammatory and antiparasitic agents [7,8], exhibit the DNA protecting activity [9], and have an effect on oncogenesis processes [8]. As a rule, the NO release from exogenic sources is related to catalytic effects of the P450 enzyme or glutathione transferase, and the involvement of endogenic thiols is required for the non-enzymatic process [10–12]. Therefore, the issue of a search for efficient exogenic sources of NO combined with the known difficulties [13–15] of NO determination both *in vivo* and *in vitro* requires the use of specific approaches towards probable mechanisms of NO-donation, in particular, quantum chemistry methods.[1]

As demonstrated by analysis of structure-property relationship, a number of furoxan derivatives with a high NO-donor activity often exist in equilibrium mixture of N_1- and N_3-oxide tautomers (Scheme 1 [9,18]).

The interrelationship of tautomers in this mixture is still unexplored but deserves careful attention, at least, for following reasons:

- Intermediate dinitroso form C can act as an independent source of NO;
- NO-donor activity might be a result of the interaction of each tautomer (A, B and C) with sulfanyl radicals RS•;
- Donating from A, B and C can occur under the UV excitation independently.

Previously we studied the processes of NO formation from furoxan, benzofuroxan and nitrobenzofuroxan derivatives induced only by such thiol-containing systems as hydrogensulfide SH^- and sulfanyl radicals RS• [16,17]. Other ways of NO donation were not considered at all. We showed that RS• radicals are responsible for nitric oxide formation and not the anions SR^- as it was commonly accepted by the community. Previous research was focused only on benzannulated systems whereas the ones annulated with quinoline were not analyzed theoretically. Thus the criteria for their structure modification remain unknown up to date. Certainly, the expansion of the number of potential NO donors based on furoxan, benzofuroxan, quionlinofuroxan derivatives will allow to reveal the receipt of systematic design of oxazole drugs.

* Corresponding author.
E-mail address: bboleg@gmail.com (O.N. Burov).

[1] Earlier, we have theoretically analyzed the mechanisms of thiol-induced transformation of furoxans yielding NO [16,17]. It was found that the formation of NO was related to the attack by HS• radical (but not by thiolate anion) of the carbon atom included in the oxadiazole ring.

https://doi.org/10.1016/j.niox.2019.08.007
Received 18 June 2019; Received in revised form 6 August 2019; Accepted 31 August 2019
Available online 06 September 2019
1089-8603/

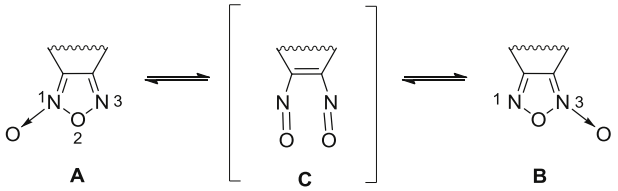

Scheme 1. Furoxans N_1,N_3-oxide tautomerism.

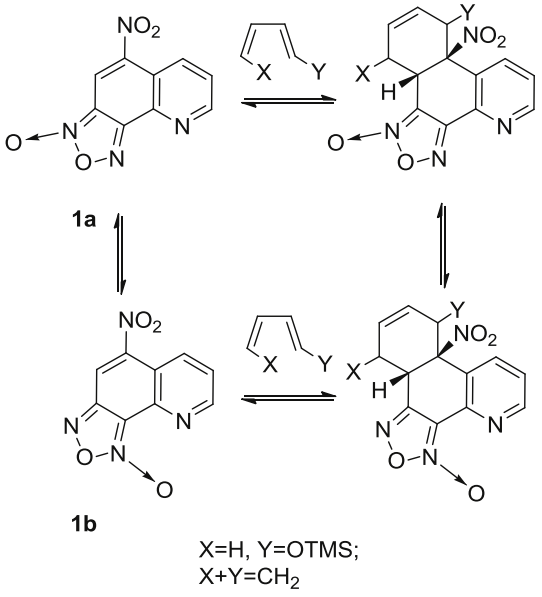

Scheme 2. 5-Nitro-7,8-furoxanoquinoline (NFQ **1**) and its [4 + 2] cycloaddition products [19,20].

Therefore, in this work we studied all possible non-enzymatic pathways of NO release from nitrofuroxanoquinoline (NFQ) derivatives.

NFQ exists as an inseparable mixture of isomers **1a** and **1b** (Scheme 2) regardless of preparation method. It's well known that isomeric products of [4 + 2] cycloaddition to its endocyclic C = C–NO_2 bond also co-exist in equilibrium [19,20]. At the same time, the effect of dearomatization processes of a six-membered carbocycles (Scheme 2) on the kinetics and thermodynamics of *N*-oxide tautomerism and possible paths of NO generation induced by these transformations, is significant.

Our previous studies have shown that the introduction of a five-membered pyrrolidine or pyrrol rings in cycloaddition reactions increases the NO-donating capacity of furoxans [9,18]. That's why the present work, at first time and thoroughly, explored [3 + 2] cycloaddition of NFQ to substituted azomethine ylide. As follows from the above, the NO-donating processes in such systems can be fundamentally influenced both by the structural features of systems (annelated rings nature and *N*-oxide tautomerism) and external factors (sulfanyl radicals attack and photoexcitation).

The effect of water solution on NO-donation can be considered insignificant, as we have shown earlier [16,17and20]. That's why we preformed quantum chemical calculations for the NFQ derivatives in the gas phase. Generally, in present study the range of investigated nitric oxide donating mechanisms have been significantly expanded. For the first time recently proposed model of sulfanyl-induced NO release was justified by *in vivo* experiment. In addition, all research methods are presented more widely: synthetic, biological and quantum chemical.

2. NO activity of NFQ

When NFQ reacts with azomethine ylide *in situ* generated from sarcosine and paraform in benzene, a mixture of isomers **2a** and **2b** in a ratio of 1:1 is produced (Scheme 3).

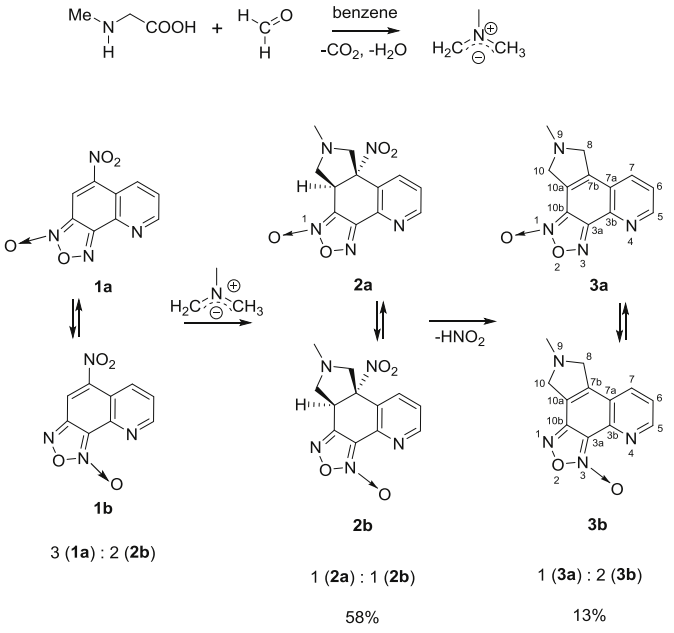

Scheme 3. 1,3-Dipolar cycloaddition of 5-nitro-7,8-furoxanoquinolines **1** to azomethine ylide and nitrous acid elimination.

Herewith, compounds **2a** and **2b** are not the sole products of cycloaddition. We isolated from the reaction mass two more species **3a** and **3b** as a non-separable mixture of isomers in a ratio of 1:2, respectively. These compounds are the result of HNO_2 elimination from cycloadducts **2a** and **2b** that leads to the aromatization of a six-membered carbocycle.[2] Different isomer ratio in the reaction products **2a** and **2b,** both in a solution[3] and the crystalline state, is of particular interest. For example, in a crystal, the ratio of isomers **2a** and **2b**, according to X-ray structural analysis, is 3:1 in favour of isomer **2a** and differs from the ratio 1:1 in solution (Scheme 3). At the same time, the ratio of isomers in products **2a** and **2b** is different from that in initial NFQ **1**, for which it is 3:2 (**1a**):(**1b**).

All of this may be related to: a) the reversible or irreversible nature of isomerization of both the original NFQ **1** and reaction products **2** and **3**; b) the different electron and spatial accessibility of the nitroolefinic coupling of **1a** and **1b** NFQ isomers for the attack by *N*-methyl azomethine ylide; and c) crystal packing effects.

Despite the fact that research mainly focuses on systems **2a** and **2b**, their precursor NFQ **1** was initially addressed. First of all, NFQ **1** is a convenient model to explore *N*-oxide equilibrium in compounds **2**. Secondly, it is crucial to understand whether isomers **2a** and **2b** originate from parallel [3 + 2] cycloaddition to isomers **1a** and **1b** or are formed purely due to the mutual transformations. Apparently, that would help understand, in which cases preparative isomers separation is possible. A close location of the *N*-oxide oxygen atom and the lone electron pair of the pyridine nitrogen atom is *a priori* a destabilizing factor, and therefore the existence of tautomer **1b** itself (and also similar tautomers **2b** and **2b**) looks pretty amazing. For instance, the recently performed quantum chemical study of *N*-oxide tautomerism of pyridinofuroxans [21] demonstrated extreme instability of one of the isomers. That is related to the spatial proximity of the *N*-oxide oxygen atom and the lone electron pair of the pyridine nitrogen atom.

[2] Similar result was earlier obtained by M.A. Bastrakov et al. in the investigations of [4 + 2] cycloaddition to NFQ [19].

[3] Signals in isomeric structures were assigned using COSY, NOESY, HMQC, HMBC spectroscopy (see Figs. S1–4 in Supplementary materials).

In order to explore the equilibrium in system **1**, we performed quantum chemical DFT calculations, according to which compound **1a** is only 0.2 kcal/mol[4] more stable than isomer **1b**, and hence should be somewhat prevailing in the mixture, which is in full agreement with experimental data.

According to calculations, single-step (concerted) tautomerism of system **1** may proceed by two competitive pathways *via* transition states **TS1** and **TS2**, which require almost the same activation energy in both cases (Scheme 4). Intermediate structures become non-equivalent resulting from rotation of the nitro group in relation to the quinoline plane by an angle of ~35° which was also found experimentally. According to X-Ray data, a deviation in the crystal reaches 57° [22].

Based on Scheme 4, one may suggest a "rearrangement from top" (**TS1**, when nitroso group is located above the plane of an aromatic fragment in transition states) and a "rearrangement from bottom" (**TS2,** when nitroso group is located below the plane).

There is also an alternative stepwise mechanism for NFQ **1** isomerization (Scheme 4) that suggests producing of the acyclic dinitroso intermediate **1c** which resembles transition states **TS3** and **TS4,** but having different mutual locations of nitroso groups. According to the calculations, the stepwise process proceeds with an activation barrier of 21.6 kcal/mol (**TS3**) *via* a kinetically unstable intermediate, that is later transformed almost without barrier into tautomer **1b**. Obviously that minimum energy pathways (MEPs) of synchronous and asynchronous processes are very close. Therefore the tautomerism of NFQ may proceed *via* both pathways simultaneously.

The direct release of the NO molecule from dinitroso form **1c** cannot be excluded (Scheme 1). This intermediate tautomer (minimum on the potential energy surface, PES) is extremely stable thermodynamically towards spontaneous release of nitric (II) oxide: from Scheme 5 one could see that this process is highly endothermic.

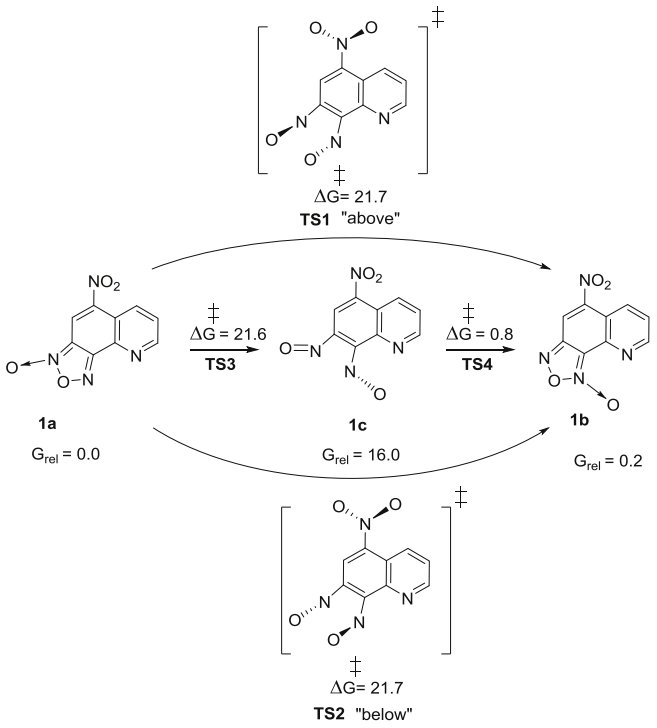

Scheme 4. NFQ **1** rearrangements. Values of G_{rel} are in kcal/mol. B3LYP/6–311 + + G(d,p) calculations.

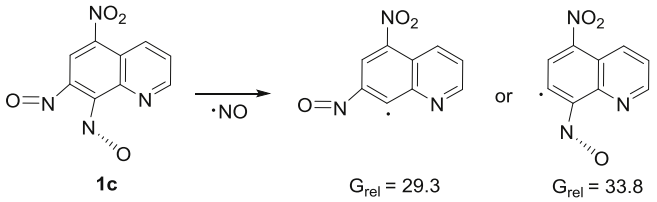

Scheme 5. Spontaneous release of NO molecule from dinitroso intermediate **1c**. Changes of relative Gibbs free energies are in kcal/mol. For the reference the free energy of system **1c** was chosen. UB3LYP/6–311 + + G(d,p) calculations.

3. NO activity of [3 + 2] adduct

The findings unambiguously suggest that both isomers **1a** and **1b** can act as direct precursors of [3 + 2] adducts **2a-b**. It is worth noting that molecules **2a** and **2b** are nonplanar, and the nitrogen atom of the pyridine fragment formed in the [3 + 2] cycloaddition is axially oriented. Comparison of quantum chemical geometric characteristics for isomers **2a** and **2b** with X-Ray data found their good agreement (Fig. 1).

Dearomatization as a consequence of cycloaddition leads to destabilization of dinitroso form and to increase in activation barriers of rearrangement **2a**⇌**2b** (Scheme 5). According to the calculations, exactly as for unsubstituted NFQ the considered isomerization may simultaneously proceed as one-step processes along two almost isoenergetic MEPs, *i.e.* from "top" ("above", **TS5**) and from "bottom" ("below", **TS6**) (Scheme 6).

We believe it is possible to explain such dramatic increase in activation barriers as follows. It is known that the activation energy of *N*-oxide isomerization of isomer **A** type is substantially reduced during transition from unsubstituted furoxan to annulated systems. This is explained by the fact that energy losses from furoxan ring expansion (~25 kcal/mol) are largely compensated (as high as 20 kcal/mol) by the restoration of benzene ring aromaticity in the intermediate structure **2c** (Scheme 6) [23,24].

Dinitroso intermediate **2c**, as well as **1c**, theoretically can undergo monomolecular decay with the formation of nitric oxide. However, according to our calculations, such a process is also highly endothermic, and therefore unrealizable spontaneously (central part of Scheme 7).

In general, dearomatization of NFQ (more precisely its benzene fragment), resulting from structural modification in [3 + 2] cycloaddition, leads to the fact that system **2** begins to behave similarly to furoxans **4** itself, and not its annulated aromatic derivatives (benzofuroxan **5** or NFQ **1**). The proximity of activation barriers of the *N*-oxide equilibrium in system **2** and unsubstituted furoxan **4**, for which the calculated activation energy of the degenerate synchronous rearrangement is 32.6 kcal/mol, proves it (Scheme 8).[5]

For comparison purposes we investigated concerted tautomerism of aromatic 10π-electron benzofuroxan **5**. As expected [24], the activation energy of the *N*-oxide equilibrium in benzofuroxan **5** is significantly lower than for non-aromatic analogue **4** (Scheme 6). The values of barriers free energies acquired for systems **4** and **5** can be considered as some sort of reference points that characterize typical non-aromatic and aromatic furoxan-containing systems, respectively.

The stepwise isomerization of system **2**, the molecular MEP of which passes through two transition states (**TS7** and **TS8**) and dinitroso intermediate **2c**, is more energetically preferred than the concerted one (Scheme 6). This proves our suggestion that intermediate **2c** can also be an NO-active substrate. Moreover, the pyrrolidine ring annulation results in enhanced activation characteristics of the stepwise process compared to the initial NFQ **1**. It is obvious that unlike tautomeric cyclization **1a**⇌**1b**, rearrangement **2a**⇌**2b** is already not tautomeric:

[4] Henceforward, that entails changes in relative values of the Gibbs free energy in kcal/mol.

[5] Experimentally measured values of the activation barrier in various non-aromatic furoxan **4** derivatives are also ~32 kcal/mol [23].

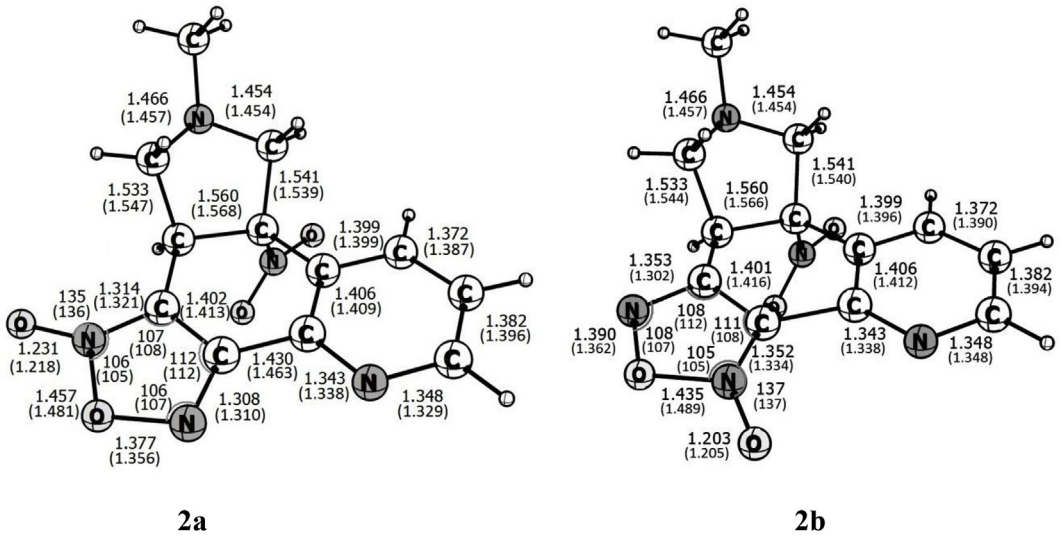

Fig. 1. Main geometric characteristics of structures **2a** and **2b**, according to X-Ray data (numbers outside brackets) and DFT-calculations in B3LYP approximations and 6–311 + + G(d,p) basis set (numbers in brackets). Interatomic distances are indicated in Angstroms, angles in degrees.

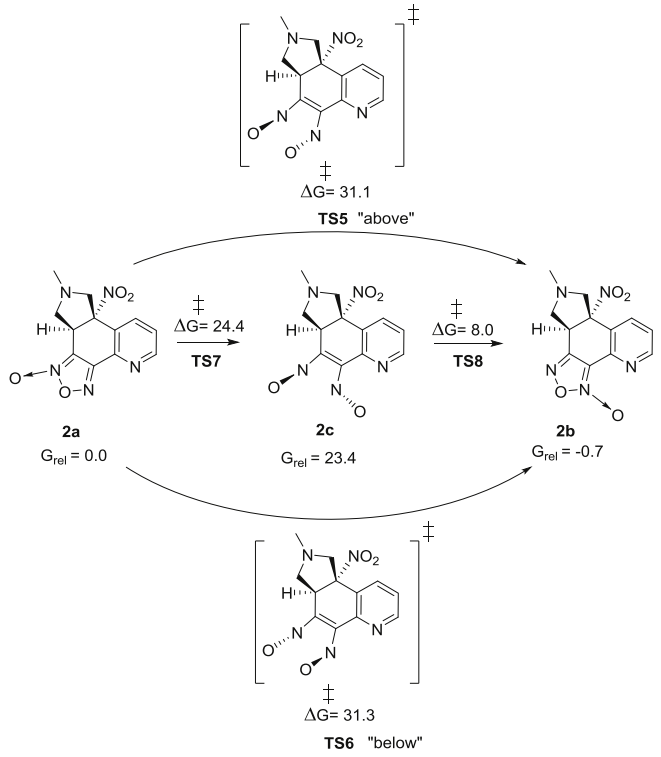

Scheme 6. Systems **2** rearrangements. Values of G_{rel} are in kcal/mol. B3LYP/6–311 + + G(d,p) calculations.

the transformation barrier is higher than 30 kcal/mol [25,26].

In summary, the calculations testify that systems **2a** and **2b** are formed not as results of intramolecular isomerization **2a**⇌**2b** but as products of independently occurring sterically inequivalent and low-barrier cycloaddition reactions of an azomethine ylide to systems **1a** and **1b** (Scheme 3) [38–40]. Herewith, the experimentally observed prevalence of isomer **2b** is highly likely to be related to the thermodynamic control of the reaction, in other words, energetic preference of **2b** compared to **2a**.

4. [3 + 2] adducts aromatization *via* HNO_2 elimination

Scheme 7 presents competitive transformation ways for [3 + 2] cycloadducts that lead to releasing of NO molecule. Among them the most actual is aromatization of cycloadducts **2a** and **2b** *via* HNO_2 elimination.

Based on these findings, decreasing the activation barrier of *N*-oxide tautomerism *via* such elimination and restoration of the six-membered ring aromaticity, looks quite clear. As expected, *N*-oxide isomerization of products **3a** and **3b** requires energy costs that are not higher than 20.6 kcal/mol (**TS13** and **TS14**). Herewith, system **3b** is somewhat more thermodynamically stable, which explains its prevalence in the reaction mixture (Scheme 9).

Like in the previously considered cases the low-barrier stepwise *N*-oxide rearrangement implies the formation of the open dinitroso form **3c** *via* transition states **TS15** and **TS16** (Scheme 9), and most likely may compete with the concerted one (**TS13, TS14**).

As demonstrated by the calculations, HNO_2 elimination proceeds with higher barriers than those for the concerted *N*-oxide rearrangement, *i.e.* 26.3 and 25.3 kcal/mol, respectively, for systems **2a** and **2b**. This additionally explains the lack of the *N*-oxide rearrangements in these adducts. This is obvious that NO elimination in these systems occurs significantly more readily than in the concerted *N*-oxide tautomerism, as the barrier of the first process is 5–6 kcal/mol lower. Thus, HNO_2 molecule that is eliminated from systems **2** is potentially a source of nitric oxide.

It should be mentioned that the removal of nitric oxide directly from intermediate **3c** is highly endothermic (Scheme 10) and not feasible spontaneously. This result is similar to obtained earlier for systems **1c**, **2c** (Scheme 5).

5. Photoinduced reactions

It is obvious that for any furoxan derivative the NO release starts from the open dinitroso structure (**1c, 2c,** or **3c**). In the case of photoinduced reactions this process must proceed through a certain excited state in which the unpaired electron occupies an antibonding hybrid orbital localized on the O–NO bond. To begin let us consider this process in NFQ **1**. The active space orbitals for compounds **1a, 1b** and **1c** obtained by SA-CASSCF(14,10). As depicted in Fig. 2, there is indeed an active antibonding orbital $\sigma(n_4)$ in NFQ localized mainly on the C–NO bond.

However, calculations of the vertical excitation spectra (SA-CASSCF

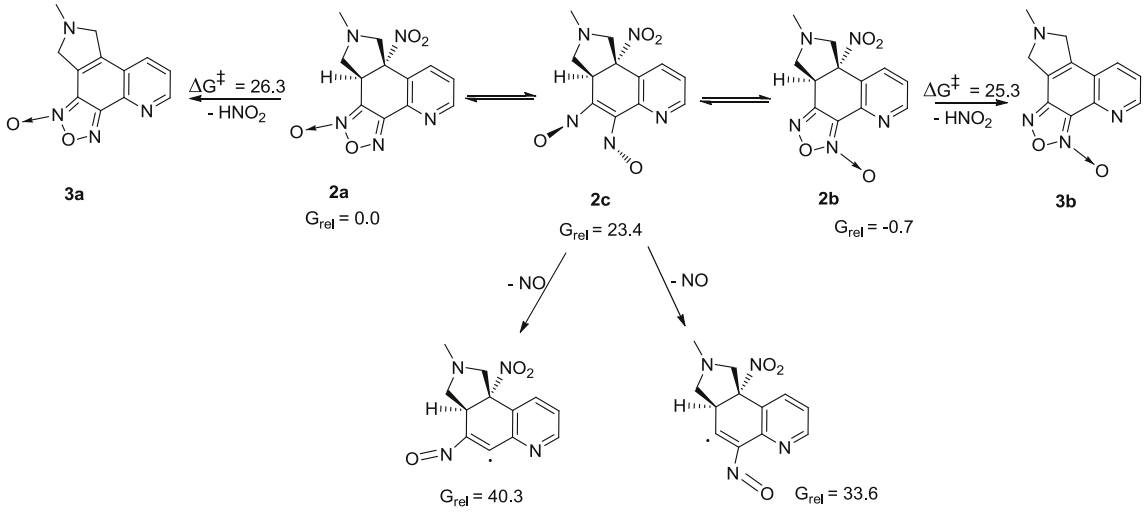

Scheme 7. NO-activity in systems **2**. Values of G_{rel} are in kcal/mol. UB3LYP/6–311 + + G(d,p) calculations.

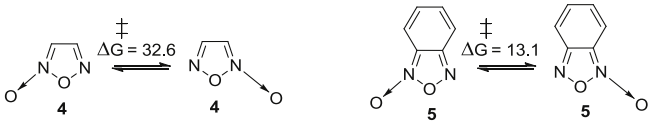

Scheme 8. Furoxan **4** and benzofuroxan **5** synchronous rearrangements. Values of G_{rel} are in kcal/mol. B3LYP/6–311 + + G(d,p) calculations.

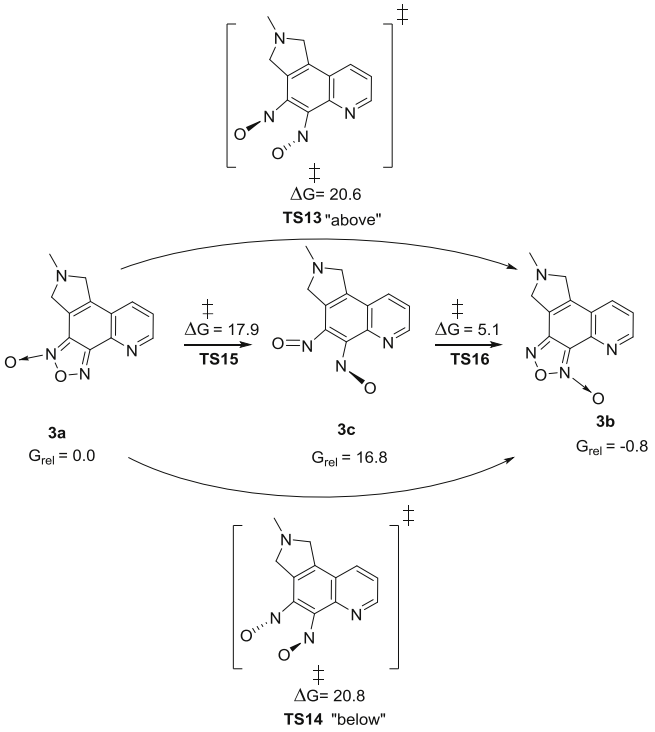

Scheme 9. Rearrangements of systems **3**. Values of G_{rel} are in kcal/mol. B3LYP/6–311 + + G(d,p) calculations.

(14.10)/6-31G(d) calculations with MP2 adjustments) have shown that the electronic state in which a given orbital would be populated by an electron is energetically unattainable when exposed to visible light or air oxygen. As shown in the diagram (Fig. 3), the vertical excitation energy in NFQ (**1a, 1b**) for states S_4 and T_4 is 6.10, 5.51 and 5.16, 5.14 eV, respectively, and the excited states correspond to the transition of the electron from the HOMO (π_4) to the hybrid orbital $\sigma(n_4)$.

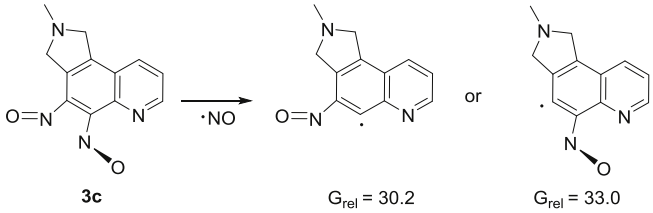

Scheme 10. Spontaneous release of NO molecule from intermediate **3c**. The changes in relative Gibbs free energies are in kcal/mol. For the reference the free energy of system **3c** was chosen. UB3LYP/6–311 + + G(d,p) calculations.

For dinitroso structure **1c** with characteristic n→π* excitation for C–NO bond cleavage two pairs of electronic states are the lowest excited [27-29]. S_1 and T_1 electronic states (1.28 and 0.73 eV, respectively) correspond to the excitation from anti-symmetric n_4-MO to π_4*-HOMO, while S_2 and T_2 (1.61 and 0.85 eV, respectively) correspond to the excitation from symmetric n_3-MO to π_4*-HOMO (MOs are depicted in Fig. S5). It also worth noting that the S_1 and T_1 electronic states refer to excitation in left nitroso group, and S_2 and T_2 – in right nitroso group (Fig. 3).

Rather low excitation energies in the NFQ dinitroso form indicate a seemingly easy achievement of the excited state and the process of NO cleavage. However, based on CAS calculations, such reactions are unrealizable due to the high kinetic instability of the open form (low energy barriers of rearrangements into NFQ **1a, 1b**) and thus a short time of life. Spontaneous decomposition of NFQ derivative **2c** is unrealizable under living organisms functioning conditions (at least, without recombination). A legitimate issue arises regarding the progression of these processes under photoirradiation conditions [30]. Analogous results were obtained for systems **2**, **3** (Figs. S5–S8, Tables S4–S9).

6. Sulfanyl induced NO release

One of the well-known and well-documented reactions of furoxans, that results in NO generation *in vivo*, is their interaction with endogenic thiols [10–12], in particular, the sulfanyl radical (HS•). As we have shown earlier [16], the formation of glutathione radical under the influence of hydroxyl radical proceeds with a gain of 34.3 kcal/mol. At the same time, the processes of the glutathione-dependent degradation of furoxans are well modelled by the sulfanil radical HS•. We have recently explored in details these processes with the involvement of various furoxans [16,17].

In the present work for systems **1**, **2** and **3** we studied only the

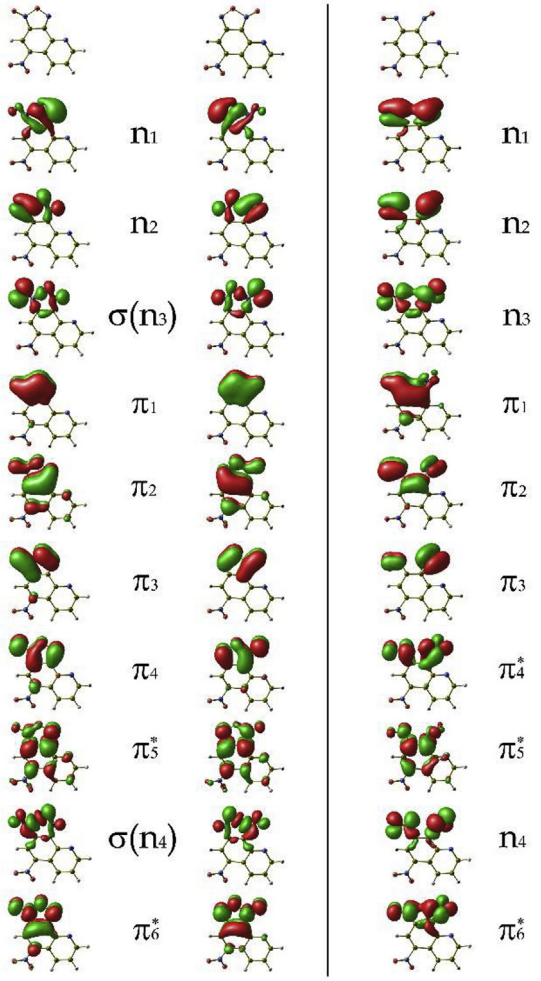

Fig. 2. MOs of systems **1a, 1b** (left) and **1c** (right). SA-CASSCF(14,10)/6-31G(d) calculations.

kinetic of initial rate determining σ-complex formation [16,17]. In system **2a** sulfanyl attack at atom C_{1a} is blocked due to a presence of H_{1b}-atom in the reaction region. The only possible for systems **2a,b** is HS• attack at atom C_{3a}. Calculations demonstrated that the attacks by HS• radicals are characterized in each case by the lowest energy costs compared to spontaneous and UV decomposition (Scheme 11). Obviously, only thiol dependent pathways can be considered as the main for nitric oxide release.

7. Biological experiments

To justify the proposed model we studied the ability of our compounds to induce SOX-operon in *E.coli* (SOX-test). In Table 1 the maximum values of the induction factor and the lowest operating concentrations for the substances synthesized are given.

It is obvious that all investigated substances are capable of inducing the SOX operon of *E.coli*. The maximum values of the induction of substances **1** and **2** are rather small, they are competing with nitroglycerin and NOC-5. At the same time, the maximum effects of substance **3** exceed those of nitroglycerin 11.7 times. The lowest concentration, for which a significant effect is noted, is 0.01 mg/ml. Thus, substance **3** are currently the undisputed leader and may be of interest for further in-depth study.

As it was pointed out in recent review, when measuring NO-activity, one should keep in mind range of mutually affecting factors, for example, presence of other highly reactive species, enzymes and accuracy of the measurement of each of them. Moreover life span of these signaling short-living radicals heavily depends on cellular redox potential. Therefore, the use of specific and sensitive methods is required in order to interpret NO signals and separate them from contribution of ther biological agents.

Modern biosensors are based on genetic engineering constructs introduced into the bacterial genome. They allow for more accurate analysis, since they are based on the quantitative detection of gene expression by bioluminescence or fluorescence and demonstrate a strict dose-response relationship for many studied factors [31,32], as well as a linear dependence on the number of cells (culture density) [33]. As it was pointed out in recent review [34], when measuring NO-activity, one should keep in mind range of mutually affecting factors, for example, presence of other highly reactive species, enzymes and accuracy of the measurement for each of them. Moreover, life span of these signaling short-living radicals heavily depends on cellular redox potential. Therefore, the use of specific and sensitive methods is required in order to interpret NO signals and separate them from contribution of other biological agents.

Therefore, the measurement of *in vivo* NO generation in real living cell, not in the electrochemical one, has the most value and predictive power among other experimental approaches to determine perspectives of NO active molecule for further study by medicinal chemistry. One of the most promising methods to the primary evaluation of new potential nitric oxide donors is the use of genetically engineered Lux-biosensors based on *E. coli*. This method makes it possible to determine quantitatively the ability of the studied compounds to induce SOX-response as a result of NO generation *in vivo* [35,36].

As we showed earlier, maximum values of the induction factor correlate with the yield of nitric oxide from furoxans detected by the EPR method in presence of sodium sulfide [37]. Results of current biological study are summarized in Table 1, and SOX-induction results are in a full accordance with quantum chemical prognosis.

For biologically leading substances **3** we studied the profile of MEP in details (Fig. 4).

From Fig. 4 it follows that the maximum barrier, as before [16,17], corresponds to the first stage (attack of the sulfanyl radicals) and does not exceed 15.5 kcal/mol. The reaction of SH• with **3b** form proceeds with smaller barriers (maximum $G^{\ddagger}_{rel}$ = 14.8 kcal/mol) and leads to a thermodynamically more stable product.

8. Conclusions

Based on the findings for NFQ and its derivatives, one can conclude that structural modification (for example in cycloaddition reactions and further HNO_2 elimination) is an effective instrument of the NO-releasing activity. Among intramolecular processes only elimination of HNO_2 has realizable energetic parameters, which nevertheless are much less favourable than for the thiol-induced mechanism. Modified NFQs themselves are not able to eliminate NO molecules. The photoirradiation acts only as NFQ tautomerism initiator and may lead to the formation of a more NO-active isomer [38].

With the NFQ structural modification we were able to get derivatives with the best NO-activity, in accordance with biological experiments. These systems were predicted by quantum chemical calculations to leaders in NO-activity in sulfanyl-induced processes.

On top of this, insight relevant for synthetic design were gained. For example, it has been convincingly demonstrated that the dearomatization observed, in particular, in cycloaddition products, dramatically increases *N*-oxide rearrangement barriers, “freezing” tautomerism, and makes it possible to separate *N*-oxides. A separation of aromatic NFQ isomers and its derivatives, produced after HNO_2 elimination, seems to be extremely difficult due to the low-barrier *N*-oxide rearrangements. At the same time, photoinitiation may be quite a useful tool to enable *N*-oxide tautomerism, which opens up new areas of the use and synthesis of the explored systems, and also their medicinal

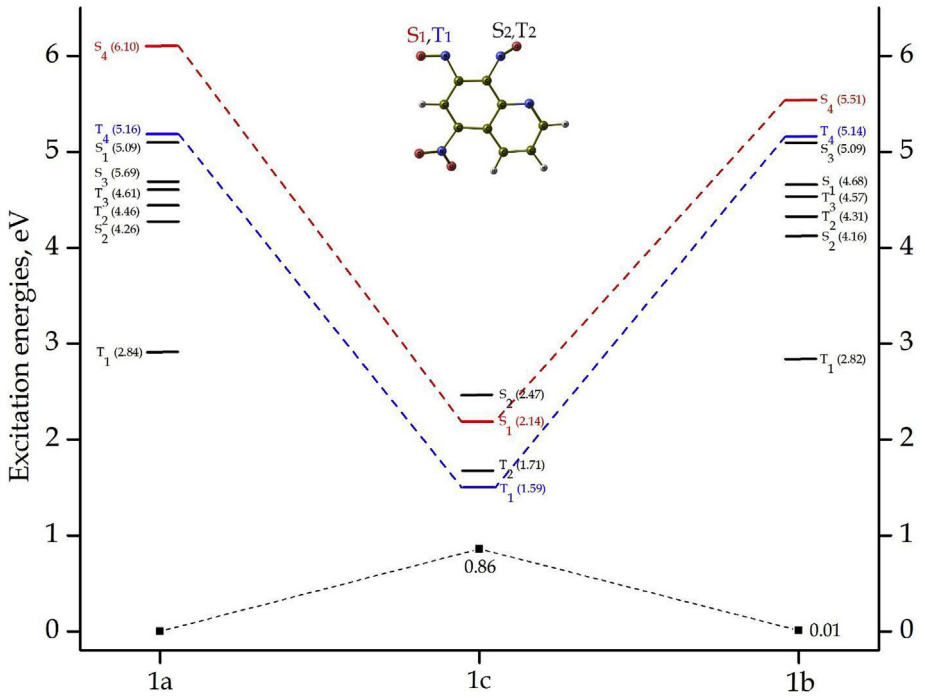

Fig. 3. Vertical excitation energies for systems **1a-c**. XMCQDPT2//CASSCF(14,10)/6-31G(d) calculations. Values of excited state energies for systems **1a-c** see in Tables S1–S3.

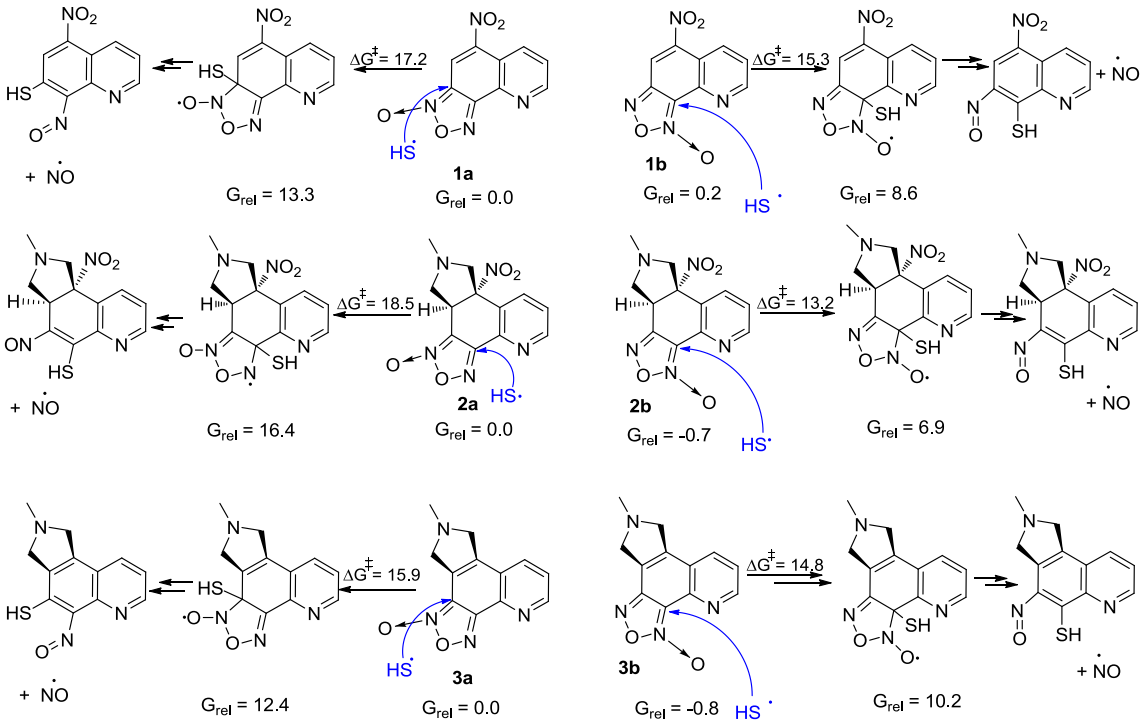

Scheme 11. Generation of NO in systems **1–3** under the sulfanyl radical (HS•) attack. UB3LYP/6–311 + +G(d,p) calculations. The changes in relative Gibbs free energies are in kcal/mol. For the reference the free energies of systems type **a** were chosen.

applications.

The most essential insights of our work allow to emphasize following trends:

1. The most energetically feasible way of NO generation proceeds through interaction of furoxan derivatives with biogenic SH• sources such as glutathione, cysteine and so on.
2. Modification of these systems in cycloaddition reactions occurring on endogenic double bonds results in formation of new highly effective NO donors.
3. Substances, in which low barrier N-oxide tautomerism is possible, are promising NO donors due to multichannel character of interactions with SH• radicals

Table 1
The maximum values of the induction factor and the lowest active concentrations of synthesized substances (SOX-test).

Substance	Concentration with a maximum value of the induction factor, mg/ml	Maximum value of the factor induction	Minimal effective concentration, mg/ml	The value of the induction factor at the minimum effective concentration
Nitroglycerin	0.1	1.90 (± 1.154)	0.001	0.048 (± 0.00857)
NOC-5	0.1	1.75 (± 0.184)	0.00001	0.977 (± 0.029)
1	0.01	1.55 (± 0.00028)	0.01	1.55
2	0.1	7.27 (± 1.237)	0.01	0.37 (± 0.121)
3	0.1	22.19 (± 1.599)	0.01	0.46 (± 0.051)

9. Experimental materials and methods

The ^{1}H and ^{13}C NMR spectra were collected on a Bruker DPX-250 NMR spectrometer (250 and 63 MHz, respectively) in $CDCl_3$; TMS was used as an internal standard. The signals were assigned through two-dimensional NMR spectroscopic analyses (COSY, NOESY, HMQC and HMBC). High resolution mass spectra (HRMS) were measured on a Bruker micrOTOF II device, electrospray ionization (ESI). The measurements were performed in a positive ion mode (interface capillary voltage - 4500 V) with a mass range from *m/z* 50 to *m/z* 3000 Da. Melting points were determined in glass capillaries using PTP device. Silica gel 60 (70–230 mesh, Merck) was used for column chromatography, A mixture of 5-nitro-[1,2,5]oxadiazolo[3,4-h]quinoline 1- and 3-oxides (**1a-b**) was synthesized according to the procedure described previously [19].

Synthesis of cycloadducts 2a-b and 3a-b. A mixture of 100 mg (0.43 mmol) of 5-nitro-[1,2,5]oxidiazolo[3,4-h]quinoline 1- and 3-oxides (**1a-b**), 192 mg (2.16 mmol) of sarcosine, 78 mg (2.59 mmol) of paraform, and 7 mL of abs. Benzene was boiled for 3 h. The reaction mass was cooled and the precipitate was filtered off, washed well with acetone, and discarded. The filtrate was evaporated in an air flow and the dry residue was subjected to SiO_2 column chromatography. Fractions with R_f = 0.75 (EtOAc eluent) and R_f = 0.28 (Me_2CO eluent) corresponding to mixtures of isomeric products **2a-b** and **3a-b**, respectively, were sequentially collected.

9-Methyl-7b-nitro-8,9,10,10a-tetrahydro-7bH-[1,2,5]oxadiazoleo[3,4-h]pyrrolo[3,4-f]quinoline 1-and 3-oxides (**2a, 2b**)**.** A mixture of isomers **2a** and **2b** in a 1:1 ratio was obtained. The yield was 72 mg (58%), colorless crystals, mp 160–162 °C. The ^{1}H NMR spectrum of isomer **2a,** δ, ppm (*J*, Hz): 2.38 (3H, s, 9-CH_3); 2.39 (1H, dd, *J* = 8.7, *J* = 9.3, 10-CH_A); 2.70 (1H, d, *J* = 11.6, 8-CH_A); 3.66 (1H, dd, *J* = 8.0, *J* = 9.3, 10-CH_B); 4.37 (1H, d, *J* = 11.6, 8-CH_B); 4.47 (1H, dd, *J* = 8.0, *J* = 8.7, 10a-CH); 7.54 (1H, dd, *J* = 4.7, *J* = 8.2, H-6); 7.95 (1H, dd*J* = 1.5, *J* = 8.2, H-7); 8.86 (1H, dd,*J* = 1.5, *J* = 4.7, H-5). The ^{13}C NMR spectrum of isomer **2a**, δ, ppm: 38.8 (C-10a); 40.7 (NCH_3); 59.0 (C-10); 67.2 (C-8); 96.0 (C-7b); 110.4 (C-10b); 126.8 (C-6); 130.2 (C-7a); 135.6 (C-7); 141.1 (C-3b); 149.9 (C-3a); 152.6 (C-5). The ^{1}H NMR spectrum of isomer **2b**, δ, ppm (*J*, Hz): 2.40 (3H, s, 9-CH_3); 2.58 (1H, dd, *J* = 8.9, *J* = 9.3, 10-CH_A); 2.76 (1H, d, *J* = 11.6, 8-CH_A); 3.67 (1H, dd, *J* = 8.4, *J* = 9.3, 10-CH_B); 4.39 (1H, d, *J* = 11.6, 8-CH_B); 4.67 (1H, dd, *J* = 8.4, *J* = 8.9, 10a-CH); 7.44 (1H, dd, *J* = 4.7, *J* = 8.2, H-6); 7.92 (1H, dd, *J* = 1.5, *J* = 8.2, H-7); 8.85 (1H, dd, *J* = 1.5, *J* = 4.7, H-5). The NMR ^{13}C spectrum of isomer **2b**, δ, ppm: 40.87 (NCH_3); 40.9 (C-10a); 61.3 (C-10); 67.3 (C-8); 96.3 (C-7b); 107.3 (C-3a); 125.2 (C-6); 128.6 (C-7a); 135.3 (C-7); 139.8 (C-3b); 152.4 (C-5); 153.1 (C-10b). Found, *m/z*: 312.0703 $[M+Na]^+$. $C_{12}H_{11}N_5NaO_4$. Calculated, *m/z*: 312.0703.

9-Methyl-9,10-dihydro-8H-[1,2,5]oxadiazole[3,4-h]pyrrolo[3,4-f]quinoline 1-and 3-oxides (**3a, 3b**)**.** A mixture of isomers **3a** and **3b** in a 1:2 ratio was obtained. The yield was 14 mg (13%), colorless crystals, mp 182–184 °C. The ^{1}H NMR spectrum of a mixture of **3a** and **3b**. δ, ppm (*J*, Hz): 2.70 (1.5H, s, 9-CH_3); 2.74 (3H, s, 9′-CH_3); 4.17–4.26 (3H, m, 8, 8′-CH_2); 4.29–4.35 (3H, m, 10, 10′-CH_2); 7.56 (1H, dd, *J* = 4.7, *J* = 8.1, H-6′); 7.65 (0.5H, dd, *J* = 4.6, *J* = 8.2, H-6); 7.85 (1H, dd, *J* = 1.7, *J* = 8.1, H-7′); 7.89 (0.5H, dd, *J* = 1.7, *J* = 8.2, H-7); 8.95–8.99 (1.5H, m, H-5, 5′). The ^{13}C NMR spectrum of isomer **3a**, δ, ppm: 42.45 (NCH_3); 58.6 (C-10); 59.7 (C-8); 110.7 (C-10b); 122.2 (C-10a); 125.6 (C-6); 126.6 (C-7a); 132.9 (C-7); 138.79 (C-7b); 140.7 (C-3b); 150.6 (C-5); 151.5 (C-3a). The ^{13}C NMR spectrum of isomer **3b**, δ, ppm: 42.53 (NCH_3); 59.0 (C-10); 60.0 (C-8); 108.9 (C-3a); 124.1 (C-6); 125.1 (C-7a); 126.4 (C-10a); 132.3 (C-7); 138.76 (C-3b); 142.3 (C-7b); 148.9 (C-10b); 150.7 (C-5). Found, *m/z*: 243.0875 $[M+H]^+$. $C_{12}H_{11}N_4O_2$. Calculated, *m/z*: 243.0877.

9.1. X-ray structural analysis

Monocrystals of cycloadducts **2a** and **2b** were produced by crystallization from a $CHCl_3$-petroleum ether (Bp 40–70 °C) mixture, 1:1 ($C_{12}H_{11}N_5O_4$, *M* = 289.26, μ = 1.17 cm^{-1}, d_{calc} = 1.509 cm^{-3}), monoclinic space group $P2_1/c$, *a* = 9.0310(10), *b* = 10.6627(10), *c* = 13.2329(14) Å, β = 92.450(2)°, *V* = 1273.1(2) $Å^3$. Intensities of

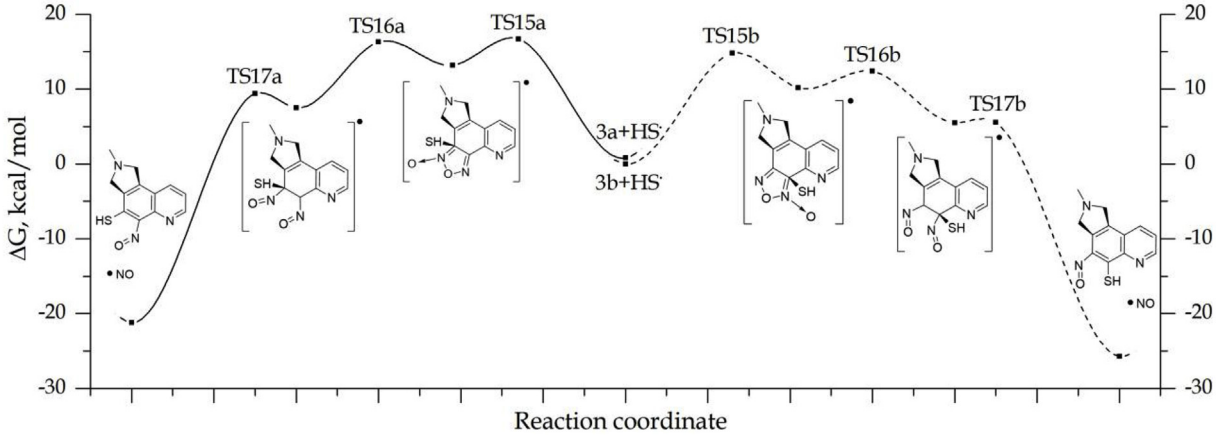

Fig. 4. MEPs for the sulfanyl induced abstraction of NO molecule in systems **3a, 3b**. UB3LYP/6–311 + + G(d,p) calculations. The changes in relative Gibbs free energies are in kcal/mol. For the reference the free energy of system type **3a** was chosen.

11697 reflections were measured on Bruker APEX II CCD diffractometer [λ(MoKa) = 0.71072 Å, ω-scans, 2θ < 56°], and 3059 independent reflections [R_{int} = 0.0210] were used for further refinement. The structure was solved by direct approach and refined by the least squares method (LSM) in the anisotropic full matrix approximation for F^2_{hkl}. As demonstrated by analysis of the difference Fourier-syntheses for electron density, and also atomic displacement parameters for furoxan ring atoms, there was no superposition of two inseparable isomers **2a** and **2b**. During furoxan fragment refinement, there were used a series of restrictions: 1) the equality of anisotropic atomic displacement parameters for pairs of the same characteristics (EADP); 2) equal bond lengths for equivalent types (DFIX). Position populations for atoms corresponding to isomers **2b** and **2a** were acquired resulting from the refinement. The former were 0.248(3) and 0.752(3). Hydrogen atomic positions were geometrically calculated and refined in the isotropic approximation. The full value of the uncertainty factor (wR_2 = 0.1539 and GOF = 1.084) for all independent reflections (R_1 = 0.0572) was computed according to F for 2641 observable reflections with $I > 2\sigma(I)$). All calculations were carried out using the SHELXTL PLUS software package [39]. Atomic coordinates and full structural data were deposited from The Cambridge Crystallographic Data Centre (CCDC 1508606).

9.2. Calculations procedure

Quantum chemical DFT calculations were carried out in the 6–311 + +G(d,p) triple-zeta basis using B3LYP [40–42] and UB3LYP [43] functionals for closed and open shells, respectively. This basis has given a good account of itself in reproduction of vibrational frequencies, geometry, and minimum energy reaction paths with the involvement of furoxan derivatives [16,17,20,44].

Full geometry optimization of molecular structures corresponding to stationary points of the potential energy surface was carried out as high as a gradient value of 10^{-7} hartree/bohr according to the Gaussian 09 software package [45] using the Silver cluster of the Research Institute of Physical and Organic Chemistry at SFedU.

The nature of stationary points was determined relying on the calculation of normal vibration frequencies (the Hessian matrix). MEPs were plotted using gradient descent from transition states in forward and reverse directions of transition vectors. In order to search for transition states, linear and quadratic synchronous transit methods were used [46,47].

CASSCF (complete active space SCF) [48,49] single-point calculations were done using Firefly QC package [50] which is partially based on the GAMESS (US) source code [51]. MP2 energy corrections for SA-CASSCF calculations were done using XMCQDPT2 method (extended multi-configuration quasi-degenerate second order perturbation theory) [52]. The 6-31G(d) basis was used for all CASSCF calculations.

The active space (AS) was chosen taking into account the methods described in Refs. [53,54]. MOs of the AS in the CASSCF calculations were characterized by the population in the range from 0.02 to 1.98. To explore the excited states of tautomers **1a-b**, **2a-b**, **3a-b** the active space comprises 14 electrons distributed in 10 orbitals (CASSCF (14, 10)) was used. Excitation energies for **1a-b**, **2a-b**, **3a-b** were calculated by state averaging over the ground and 8 low lying excited states with equal weights for each state (SA9-CASSCF (14,10)). Excitation energies for **1c**, **2c**, **3c** were calculated by state averaging over the ground and 4 low lying excited states with equal weights for each state (SA5-CASSCF (14, 10)).

9.3. Materials and methods of biological experiments

SOX-test. For the primary activity screening, we used the property of nitric oxide to induce SOX-operon induction in *E.coli*. As is known, SoxR protein, normally associated with pSoxS promoter, triggers expression of genes united in SOX-operon. This process starts after its domain containing iron-sulfur clusters interacts with either superoxide-anion radical (in this case, there is a reduction of FeS groups), or with nitrogen oxide (in this case, there is nitrosylation of FeS groups) [55].

To detect the ability of the studied substances to induce SOX-operon, a genetically engineered biosensor *E.coli* MG 1655 (pSoxS-lux) was used, created on the basis of the strain *E. coli* MG1655. It was done by introducing a plasmid constructed in Refs. [56–58] with the operon lux CDABE *Photorhabdus luminescens* photo bacteria, which was placed under the control of the pSoxS promoter.

This genetic design responds by increasing the luminescence to the presence of nitrogen oxide or superoxide-anion radical in the medium of generators.

Samples preparation. The analyzed compounds were dissolved in acetone up to 10 mg/ml, then a series of successive dilutions in deionized water up to 10^{-4} mg/ml were made from this solution. Thus the following concentrations of substances were tested: 1.0; 0.1; 0.01; 0.001; 0.0001; 0.00001 mg/ml. As a control for each dilution, acetone solution in deionized water was used in a concentration similar to the corresponding dilution.

Bioluminescence. *E.coli* cells cultures were grown on a full-fledged Luria-Bertani (LB) medium [59,60]. Cultivation of bacteria in a liquid nutrient medium was carried out at a constant aeration on a circular rocking at 30 °C. LB-agar (LB + 20 g/liter of microbiological agar) was used for growing on a solid medium. The antibiotic ampicillin (100 μg/ml) was added to both liquid and solid media.

Cultivation of bacteria in a liquid culture medium was carried out at 37 °C to an early or medium logarithmic phase. Night culture was diluted with fresh medium to a density of 0.01, 0.1 and 1 unit of MacFarland (concentrations $3{\cdot}10^8$–$3{\cdot}10^6$ cells/ml) for *E.coli* strain MG 1655 (pSoxS-lux).

Measurements were carried out using DEN-1B densitometer (Biosan, Lithuania). The suspension was then grown for 2 h before the early logarithmic phase. Aliquots of this culture (90 μl each) were transferred to sterile cells located in strips of a 96-well plate for a luminometer, and 10 μl of the tested drug were added to them. 10 μl of deionized water were added to the control cells.

Luminescence measurements. After treatment, the plate with samples was placed in a luminometer and incubated at 30 °C. Bioluminescence intensity was measured every 10–15 min. The LM-01T microplate luminometer (Immunotech, Czech Republic) was used for luminescence measurements. The SOS response induction factor (I^s) was calculated by the formula:

$$I^S = \frac{L_e}{L_k} - 1 \quad (1)$$

where.

L_k – luminescence intensity of the control sample (in conventional units)

L_e is the intensity of luminescence of the experimental sample (in conventional units).

Statistically significant excess of L_e over L_k estimated by t-criterion was considered as a sign of reliability of SOS-induction effect.

Acknowledgments

The study was carried out by support of the Southern Federal University. Also we want to express our gratitude to E.Y. Kharchenko for the biological experiments.

Appendix A. Supplementary data

Supplementary data to this article can be found online at https://doi.org/10.1016/j.niox.2019.08.007.

References

[1] P.G. Wang, T.B. Cai, N. Taniguchi, Nitric Oxide Donors: for Pharmaceutical and Biological Applications, Wiley-VCH, 2005.
[2] L.J. Ignarro, Nitric Oxide: Biology and Pathobiology, Academic Press, San Diego, CA, 2000.
[3] V.G. Granik, N.B. Grigoriev, Oxide of Nitrogen (NO). A New Way to Search of Medicines, The High school book, Moscow, 2004.
[4] H. Cerecetto, W. Porcal, Pharmacological properties of furoxans and benzofuroxans: recent developments, Mini Rev. Med. Chem. 5 (2005) 57–71.
[5] M.R. Miller, I.L. Megson, Recent developments in nitric oxide donor drugs, Br. J. Pharmacol. 151 (2007) 305–321.
[6] C. Jovene, E.A. Chugunova, R. Goumont, The properties and the use of substituted benzofuroxans in pharmaceutical and medicinal chemistry: a comprehensive review, Mini Rev. Med. Chem. 13 (2013) 1089–1136.
[7] G.F. dos, S. Fernandes, P.C. de Souza, L.B. Marino, K. Chegaev, S. Guglielmo, L. Lazzarato, R. Fruttero, M.C. Chung, F.R. Pavan, J.L. dos Santos, Synthesis and biological activity of furoxan derivatives against Mycobacterium tuberculosis, Eur. J. Med. Chem. 123 (2016) 523–531.
[8] M. Amir, M.W. Akhter, T. Sana, S. Kanagasabai, Furoxan derivatives as nitric oxide donors and their therapeutic potential, Int. Res. J. Pharm. 6 (2015) 585–599.
[9] V.A. Chistyakov, Y.P. Semenyuk, P.G. Morozov, E.V. Prazdnova, V.K. Chmykhalo, E.Y. Kharchenko, M.E. Kletskii, G.S. Borodkin, A.V. Lisovin, O.N. Burov, S.V. Kurbatov, Synthesis and biological properties of nitrobenzoxadiazole derivatives as potential nitrogen(II) oxide donors: SOX induction, toxicity, genotoxicity, and DNA protective activity in experiments using Escherichia coli-based lux biosensors, Russ. Chem. Bull. 64 (2015) 1369–1377.
[10] M. Feelish, K. Shönafinger, E. Noack, Thiol-mediated generation of nitric oxide accounts for the vasodilator action of furoxans, Biochem. Pharmacol. 44 (1992) 1149–1157.
[11] C. Medana, G. Ermondi, R. Fruttero, A. Di Stilo, C. Ferretti, A. Gasco, Furoxans as nitric oxide donors. 4-phenyl-3-furoxancarbonitrile: thiol-mediated nitric oxide release and biological evaluation, J. Med. Chem. 37 (1994) 4412–4416.
[12] C.M. Turnbull, C. Cena, R. Fruttero, A. Gasco, A.G. Rossi, I.L. Megson, Mechanism of action of novel NO-releasing furoxan derivatives of aspirin in human platelets, Br. J. Pharmacol. 148 (2006) 517–526.
[13] T. Nagano, T. Yoshimura, Bioimaging of nitric oxide, Chem. Rev. 102 (2002) 1235–1269.
[14] M.H. Lim, D. Xu, S.J. Lippard, Visualization of nitric oxide in living cells by a copper-based fluorescent probe, Nat. Chem. Biol. 2 (2007) 375–380.
[15] K.-J. Huang, H. Wang, M. Ma, X. Zhang, H.-Sh Zhang, Real-time imaging of nitric oxide production in living cells with 1,3,5,7-tetramethyl-2,6-dicarbobethoxy-8-(3'-4'-diaminophenyl)-difluoroboradiaza-s-indacence by invert fluorescence microscope, Nitric Oxide 16 (2007) 34–43.
[16] O.N. Burov, M.E. Kletskii, N.S. Fedik, A.V. Lisovin, S.V. Kurbatov, Mechanism of thiol-induced nitrogen(II) oxide donation by furoxans: a quantum-chemical study, Chem. Heterocycl. Comp. 51 (2015) 951–960.
[17] M.E. Kletskii, O.N. Burov, N.S. Fedik, S.V. Kurbatov, Thiol-induced nitric oxide donation mechanisms in substituted dinitrobenzofuroxans, Nitric Oxide 62 (2017) 44–51.
[18] E.V. Prazdnova, E.Y. Kharchenko, V.A. Chistyakov, YuP. Semenyuk, P.G. Morozov, S.V. Kurbatov, V.K. Chmyhalo, Synthesis and biological properties of new nitrobenzoxadiazole derivatives, BLM 7 (2015) 3.
[19] M.A. Bastrakov, A.M. Starosotnikov, I.V. Fedyanin, V.V. Kachala, S.A. Shevelev, 5-Nitro-7,8-furoxanoquinoline: a new type of fused nitroarenes possessing Diels-Alder reactivity, Mendeleev Commun. 24 (2014) 203–205.
[20] D.V. Steglenko, S.A. Shevelev, M.E. Kletskii, O.N. Burov, A.V. Lisovin, A.M. Starosotnikov, P.G. Morozov, S.V. Kurbatov, V.I. Minkin, M.A. Bastrakov, Quantum-chemical and NMR study of nitrofuroxanoquinoline cycloaddition, Chem. Heterocycl. Comp. 51 (2015) 838–844.
[21] S. Vega-Rodríguez, R. Jiménez-Cataño, E. Leyva, Tautomerism in substituted pyridofuroxans: a theoretical study, Comput. Theor. Chem. 1090 (2016) 105–111.
[22] http://zioc.ru/files/Starosotnikov_diss.pdf , Accessed date: August 2018.
[23] A. Gasco, A.J. Boulton, Furazans and furazan oxides. Part IV. The structures and tautomerism of some unsymmetrically substituted furoxans, J. Chem. Soc. Perkin Trans. 2 (12) (1973) 1613–1617.
[24] K.-I. Dahlqvist, S. Forsén, Application of density matrix methods to the study of spin exchange II. Evaluation of the interconversion barrier in benzofuroxan, J. Magn. Reson. 2 (1970) 61–68.
[25] G. Schneider, K.-H. Baringhaus, H. Kubinyi, Molecular Design: Concepts and Application, Wiley-VCH, 2008.
[26] V.I. Minkin, L.P. Olekhnovich, YuA. Zhdanov, Molecular Design of Tautomeric Compounds, D. Reidel Publishing Company, Dordrecht, 1998.
[27] E. Runge, E.K.U. Gross, Density-Functional theory for time-dependent systems, Phys. Rev. Lett. 52 (1984) 997–1000.
[28] C.M. Tseng, Y.M. Choi, C.L. Huang, C.K. Ni, Y.T. Lee, M.C. Lin, Photodissociation of nitrosobenzene and decomposition of phenyl radical, J. Phys. Chem. A 108 (2004) 7928–7935.
[29] M.E. Kletskii, A.V. Lisovin, O.N. Burov, S.V. Kurbatov, Competing mechanisms of Norrish and Norrish-like reactions in a wide range of systems - from carbonyl compounds to nitrogen oxide donators, Comput. Theor. Chem. 1047 (2014) 55–66.
[30] K.-J. Hwang, S.K. Kim, S.Ch Shim, Photochemical generation of nitric oxide from 3,4-Bis-2'-chlorophenylfuroxan, Chem. Lett. (1998) 859–860.
[31] C. Lu, C.R. Albano, W.E. Bentley, G. Rao, Quantitative and kinetic study of oxidative stress regulons using green fluorescent protein, Biotechnol. Bioeng. 89 (5) (2005) 574–587.
[32] G.B. Zavilgelsky, V.Y. Kotova, I.V. Manukhov, Action of 1, 1-dimethylhydrazine on bacterial cells is determined by hydrogen peroxide, Mutat. Res. Genet. Toxicol. Environ. Mutagen. 634 (1–2) (2007) 172–176.
[33] L.D. Rasmussen, R.R. Turner, T. Barkay, Cell-density-dependent sensitivity of a merlux bioassay, Appl. Environ. Microbiol. 63 (8) (1997) 3291–3293.
[34] A. Vishwakarma, A. Wany, S. Pandey, M. Bulle, A. Kumari, R. Kishorekumar, A.U. Igamberdiev, L.A.J. Mur, K.J. Gupta, Current approaches to measure nitric oxide in plants, J. Exp. Bot. 70 (17) (2019) 4333–4343, https://doi.org/10.1093/jxb/erz242 pii: erz242.
[35] V.A. Chistyakov, YuP. Semenyuk, P.G. Morozov, E.V. Prazdnova, V.K. Chmykhalo, E.Yu Kharchenko, M.E. Kletskii, G.S. Borodkin, A.V. Lisovin, O.N. Burov, S.V. Kurbatov, Synthesis and biological properties of nitrobenzoxadiazole derivatives as potential nitrogen(II) oxide donors: SOX induction, toxicity, genotoxicity, and DNA protective activity in experiments using Escherichia colibased lux biosensors, Russ. Chem. Bull. 64 (2015) 1369.
[36] E.V. Prazdnova, E.Y. Kharchenko, V.A. Chistyakov, YuP. Semenyuk, P.G. Morozov, S.V. Kurbatov, V.K. Chmyhalo, Synthesis and biological properties of new nitrobenzoxadiazole derivatives, Biol. Med. 7 (2015) 2.
[37] V.A. Serezhenkov, N.A. Tkachev, YuP. Semenyuk, S.V. Kurbatov, E.Yu Kharchenko, V.A. Chistyakov, Nitrobenzoxadiazole derivatives as nitric oxide donors: ESR study using spin trapping, Russ. Chem. Bull. Int. Ed. 66 (2017) 76–82.
[38] R. Matsubara, S. Takazawa, A. Ando, M. Hayashi, R. Tohda, M. Tsubaki, Study on the photoinduced nitric-oxide-releasing ability of 4-alkoxy furoxans, Asian J. Org. Chem. 6 (2017) 619–626.
[39] G.M. Sheldrick, A short history of SHELX, Acta Crystallogr. A 64 (2008) 112–122.
[40] A.D. Becke, Density-functional exchange-energy approximation with correct asymptotic behavior, Phys. Rev. A 15 (1988) 3098–3100.
[41] A.D. Becke, Density-functional thermochemistry. III. The role of exact exchange, J. Chem. Phys. 98 (1993) 5648–5652.
[42] Ch Lee, W. Yang, R.G. Parr, Development of the Colle-Salvetti correlation-energy formula into a functional of the electron density, Phys. Rev. B. 37 (1988) 785–789.
[43] W.J. Hehre, L. Radom, P.v.R. Schleyer, J.A. Pople, Ab Initio Molecular Orbital Theory, Wiley Interscience, New York, 1986.
[44] Ya-J. Peng, Y.-X. Jiang, X. Peng, J.-Y. Liu, W.-P. Lai, Reaction mechanism of 3,4-dinitrofuroxan formation from glyoxime: dehydrogenation and cyclization of oxime, ChemPhysChem 17 (2016) 541–547.
[45] Gaussian 09, M.J. Frisch, G.W. Trucks, H.B. Schlegel, G.E. Scuseria, M.A. Robb, J.R. Cheeseman, G. Scalmani, V. Barone, B. Mennucci, G.A. Petersson, H. Nakatsuji, M. Caricato, X. Li, H.P. Hratchian, A.F. Izmaylov, J. Bloino, G. Zheng, J.L. Sonnenberg, M. Hada, M. Ehara, K. Toyota, R. Fukuda, J. Hasegawa, M. Ishida, T. Nakajima, Y. Honda, O. Kitao, H. Nakai, T. Vreven, J.A. Montgomery, Jr, J.E. Peralta, F. Ogliaro, M. Bearpark, J.J. Heyd, E. Brothers, K. N. Kudin, V.N. Staroverov, R. Kobayashi, J. Normand, K. Raghavachari, A. Rendell, J.C. Burant, S.S. Iyengar, J. Tomasi, M. Cossi, N. Rega, J.M. Millam, M. Klene, J.E. Knox, J.B. Cross, V. Bakken, C. Adamo, J. Jaramillo, R. Gomperts, R.E. Stratmann, O. Yazyev, A.J. Austin, R. Cammi, C. Pomelli, J.W. Ochterski, R.L. Martin, K. Morokuma, V.G. Zakrzewski, G.A. Voth, P. Salvador, J.J. Dannenberg, S. Dapprich, A.D. Daniels, O. Farkas, J.B. Foresman, J.V. Ortiz, J. Cioslowski, and D.J. Fox, Gaussian, Inc., Wallingford CT, 2009.
[46] C. Peng, H.B. Schlegel, Combining synchronous transit and quasi-Newton methods to find transition states, Isr. J. Chem. 33 (1993) 449–454.
[47] C. Peng, P.Y. Ayala, H.B. Schlegel, M.J. Frisch, Using redundant internal coordinates to optimize equilibrium geometries and transition states, J. Comput. Chem. 17 (1996) 49–56.
[48] H.-J. Werner, Matrix-formulated direct multiconfiguration self-consistent field and multiconfiguration reference configuration-interaction methods, Adv. Chem. Phys. 69 (1987) 1–62.
[49] B.O. Roos, The complete active space self-consistent field method and its applications in electronic structure calculation, Adv. Chem. Phys. 69 (1987) 399–445.
[50] A.A. Granovsky, Firefly version 8, http://www.classic.chem.msu.su/gran/firefly/index.html (accessed November 2014).
[51] M.W. Schmidt, K.K. Baldridge, J.A. Boatz, S.T. Elbert, M.S. Gordon, J.H. Jensen, S. Koseki, N. Matsunaga, K.A. Nguyen, S. Su, T.L. Windus, M. Dupuis, J.A. Montgomery, General atomic and molecular electronic structure system, J. Comput. Chem. 14 (1993) 1347–1363.
[52] A.A. Granovsky, Extended multi-configuration quasi-degenerate perturbation theory: the new approach to multi-state multi-reference perturbation theory, J. Chem. Phys. 134 (2011) 214113.
[53] C.J. Cramer, Essentials of Computational Chemistry, John Wiley & Sons Ltd, Chichester, 2004.
[54] F. Jensen, Introduction to Computational Chemistry, John Wiley & Sons Ltd, Chichester, 2007.
[55] H. Ding, B. Demple, Direct nitric oxide signal transduction *via* nitrosylation of iron-sulfur centers in the SoxR transcription activator, Proc. Nat. Acad. Sci. USA. 97 (2000) 5146–5150.
[56] I.V. Manukhov, G.E. Eroshnikov, M.Yu Vissokikh, G.B. Zavilgelsky, Folding and refolding of thermolabile and thermostable bacterial luciferases: the role of DnaKJ heat-shock proteins, FEBS Lett. 448 (1999) 265–268.
[57] E.V. Prazdnova, S.V. Dem'yanenko, V.A. Chistyakov, V.S. Lysenko, M.M. Batyushin, Carotenoids-antioxidants of *D.radiodurans* stimulate regeneration in mice, Biol. Med. 6 (2014) 1–6.
[58] G.B. Zavilgelsky, V.Yu Kotova, I.V. Manukhov, Action of 1,1-dimethylhydrazine on bacterial cells is determined by hydrogen peroxide, Mutat. Res. 634 (2007) 172–176.
[59] T. Maniatis, E. Fritsch, J. Sambrook, Methods of Genetic Engineering. Molecular Cloning, Mir, Moscow, 1984, p. 480.
[60] Guidelines for susceptibility testing of microorganisms to antibacterial agents, Clin. Microbiol. Antimicrob. Chemother. 6 (2004) 306–359 (in Russian).